Environmental Science & Technology

Article

pubs.acs.org/est

Transport of Oxidized Multi-Walled Carbon Nanotubes through Silica Based Porous Media: Influences of Aquatic Chemistry, Surface Chemistry, and Natural Organic Matter

Jin Yang,[†] Julie L. Bitter,[‡] Billy A. Smith,[‡] D. Howard Fairbrother,[‡] and William P. Ball*[,†]

[†]Department of Geography and Environmental Engineering, and [‡]Department of Chemistry, Johns Hopkins University, Baltimore, Maryland 21218, United States

Supporting Information

ABSTRACT: This paper provides results from studies of the transport of oxidized multi-walled carbon nanotubes (O-MWCNTs) of varying surface oxygen concentrations under a range of aquatic conditions and through uniform silica glass bead media. In the presence of Na^+, the required ionic strength (IS) for maximum particle attachment efficiency (*i.e.*, the critical deposition concentration, or CDC) increased as the surface oxygen concentration of the O-MWCNTs or pH increased, following qualitative tenets of theories based on electrostatic interactions. In the presence of Ca^{2+}, CDC values were lower than those with Na^+ present, but were no longer sensitive to surface oxygen content, suggesting that Ca^{2+} impacts the interactions between O-MWCNTs and glass beads by mechanisms other than electrostatic alone. The presence of Suwannee River natural organic matter (SRNOM) decreased the attachment efficiency of O-MWCNTs in the presence of either Na^+ or Ca^{2+}, but with more pronounced effects when Na^+ was present. Nevertheless, low concentrations of SRNOM (<4 mg/L of dissolved organic carbon) were sufficient to mobilize all O-MWCNTs studied at $CaCl_2$ concentrations as high as 10 mM. Overall, this study reveals that NOM content, pH, and cation type show more importance than surface chemistry in affecting O-MWCNTs deposition during transport through silica-based porous media.

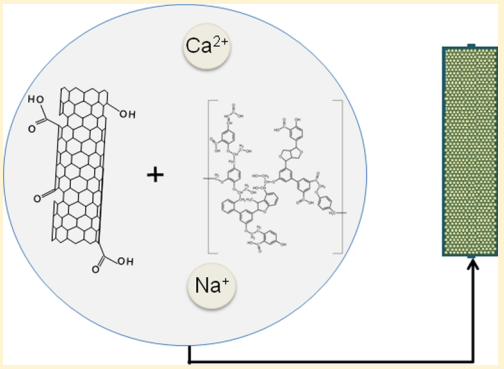

INTRODUCTION

Carbon nanotubes (CNTs), with their unique structure and properties,[1−5] have a widespread range of current and potential applications,[6] and their production rates have steadily increased over the past decade.[7] Multi-walled CNTs (MWCNTs) cost less to produce and are sold in much greater quantities than single-walled CNTs (SWCNTs),[7] with correspondingly higher potential for environmental release. Although pathways for release have not yet been well established,[8−10] it is reasonable to assume that aqueous contamination may occur as the result of direct emissions to air or water through spills or misuse and also perhaps following long-term degradation of the commercial materials into which CNTs are embedded.[8−10] MWCNT surfaces are often oxidized during production to increase their stability in water or polar solvents used with some polymeric resins,[11−16] or to improve their properties for use as drug delivery agents.[17] Surface oxides can also be introduced onto MWCNTs inadvertently during purification with acids or through exposure to UV radiation, reactive radicals, and/or ozone.[18−20] The existence of such oxides on MWCNT surfaces have been shown to dramatically influence environmentally relevant properties, such as homoaggregation and sorption, in aquatic environments.[21−23]

To better understand MWCNT transport in groundwater or engineered processes of filtration it is useful to consider well-studied physical and chemical principles of colloid transport through porous media.[24−46] Chemical interactions between suspended particles and environmental collectors include London−van der Waals forces, electrostatic interactions, hydration forces, and steric interactions[24−36,38−41] as well as some specific short-range interactions, such as the so-called "bridging" effects of Ca^{2+} with carboxylic groups.[42−46] All of these interactions are intimately dependent on surface and solution chemistry and have been extensively studied in prior works.[44−50] In prior studies of particle retention in porous media, researchers have found it useful to separately consider the case of "clean bed filtration" in which particle interactions with the solid media ("collectors") are studied under conditions in which (1) the volume of particles (colloids) removed is low enough that collector surfaces have been negligibly covered, and (2) substantial amounts of straining are avoided. Here, we follow numerous others by defining straining as the "trapping of colloids in pore throats that are too small to allow their passage".[51] The avoidance of substantial amounts of straining helps to ensure depth filtration and is important for

Received: June 3, 2013
Revised: November 14, 2013
Accepted: November 19, 2013
Published: November 19, 2013

experimental studies where the goal is to isolate and understand the relative roles of collision efficiency, η_0, and attachment efficiency, α, as separate components of a first-order deposition rate coefficient, k_d, that has been traditionally formulated in terms of the product $\alpha\eta_0$ and other coefficients that are constant for a given pore water velocity and porous media type.[24,25,38] In such a formulation, η_0 represents the fraction of approaching particles that can theoretically result in collision (due to interception, sedimentation, and diffusion) and α represents the number of actual colloid-collector attachments that occur for a given number of collision opportunities.

Given the unique structure of MWCNTs, especially their small diameters, high aspect ratios, and varied surface chemistry, it is difficult to estimate η_0 from theory or to extrapolate its value from previous studies with other materials. Within this context, and to the best of our knowledge, no prior studies have specifically addressed the issue of surface oxygen and water chemistry impacts on deposition rate coefficients and attachment efficiencies during oxidized MWCNT (O-MWCNT) transport through clean beds. In the study reported herein we focused on this issue through the estimation of attachment efficiencies between the glass surfaces of spherical filter "collectors" and the surfaces of individual O-MWCNTs of varying surface composition. Estimation on attachment efficiency is made possible through well-controlled conditions of transport under conditions that were designed to ensure so-called "clean bed filtration," to which first-order irreversible removal rates apply for the majority of the observed fractional removal, as independently verified through spatial retention profiles and model simulation.

Although several prior studies have investigated CNT transport through porous media, most studies to date have been conducted with natural soil or quartz sand systems and none have quantified attachment efficiency as a function of both surface and solution chemistry. Moreover, given that size heterogeneity and surface roughness of the porous media tend to enhance straining,[51] it is not surprising that most prior work has been influenced by straining effects. For example, in their studies of the transport of oxidized SWCNTs through quartz sand as a function of ionic strength (IS), Jaisi et al.[52,53] found that O-SWCNT transport followed predictions of conventional deposition theory under most conditions for quartz sand[52] but that straining was the primary means of O-SWCNT deposition with soils under all conditions.[53] In their study of functionalized MWCNT tube-length effects on transport through quartz sand, Wang et al.[54] also reported that that straining played an important role—these investigators observed spatial retention profiles that deviated substantially from expectations based on simple first-order removal and attachment efficiencies could not be estimated. Other researchers have investigated the impact of CNT tube diameter[55] and flow velocity[56] on transport through quartz sand (and glass beads for flow velocity test) but these studies also did not focus on quantifying attachment efficiency.

Prior studies of solution chemistry effects on O-MWCNT surface properties in water have primarily focused on homoaggregation (see Chen et al. for a review[57]), with relatively few studies conducted in transport systems. The prior homoaggregation work has revealed a major impact of pH and ionic strength that is qualitatively consistent with Derjaguin–Landau–Verwey–Overbeek (DLVO) theory[21,58] as well as some important effects of calcium and natural organic matter (NOM). The effect of surface chemistry on the homoaggregation of O-MWCNTs has also been studied.[21,42] For example, Hyung et al.[59] reported that for any given mass of added MWCNT powder, the concentration of well-dispersed MWCNTs in solution increased systematically with concentration of Suwannee River natural organic matter (SRNOM). Prior work in our own laboratory[42] has revealed that NOM concentrations as low as 0.5 mg of dissolved organic carbon (DOC)/L can significantly enhance the stability of O-MWCNT dispersions and that these effects occur even in the presence of Ca^{2+} and in a manner largely independent of O-MWCNT surface oxygen concentration. Although the effect of aquatic chemistry and surface chemistry on CNT homoaggregation has been widely reported,[25,41,42,47,48,60−64] such effects on CNT attachment to other media during transport have been less well studied. Wang et al.[64] passed NOM-stabilized MWCNT and SWCNT dispersions through sand packed columns at varied KCl and $CaCl_2$ concentrations and observed that substantial mass fractions of CNTs passed through the column at KCl concentrations up to 1 mM and $CaCl_2$ up to 0.1 mM. Jaisi et al.[52] have reported that the presence of NOM can substantially decrease rates of SWCNT deposition onto quartz sand in the presence Ca^{2+}. Yi et al.[43] have studied deposition of MWCNTs with two different surface oxygen concentrations on quartz crystals, but did not study transport through packed columns.

In the study reported herein, we focused on quantifying the impacts of surface and solution chemistry on O-MWCNT attachment efficiency with amorphous silica surfaces during transport through porous media. It is noteworthy that our own focus was on *relative* alpha values as a reflection of the effects of aquatic chemistry and O-MWCNT surface chemistry, for a *consistently reproducible* media surface. To accurately measure attachment efficiencies in the absence of substantial straining effects, we used a well-defined system of uniformly sized spherical collectors and, to ensure "clean-bed" filtration conditions, we used very small input masses of CNTs. To enhance experimental reproducibility, we used rigorous and standardized methods of media cleaning. Studies were conducted on O-MWCNTs with five different oxygen contents in varied solution chemistry. Solution chemistry variables included ionic strength, pH, type of cations in the feed solution (sodium or calcium), and concentration of SRNOM.

EXPERIMENTAL PROCEDURES

Surface Oxidation, Characterization, and Preparation of Colloidal O-MWCNTs. MWCNTs with diameters of 15 ± 5 nm and lengths of 1−5 μm were purchased from NanoLabs, Inc. Details regarding our methods for oxidation and characterization of these materials and preparation of O-MWCNT dispersions have been provided in previous papers[21,57,65−70] and are briefly summarized in the Supporting Information (SI), including Table S1 and Table S2.

Preparation of Suwannee River Natural Organic Matter (SRNOM). SRNOM was purchased from the International Humic Substances Society. After dissolution into DI water the SRNOM was passed through a 0.22 μm polyethersulfone filter (EMD Millipore Corporation). The filtered stock solution was analyzed for total organic carbon content (Dohrmann 8000). This stock solution was subsequently diluted for calibration of DOC against UV absorbance at 254 nm and for preparation of various column feed solutions containing SRNOM concentrations between 0 and 4.1 mg of DOC/L.

Preparation of Glass Beads and Packed Columns. Soda lime glass spheres (0.355−0.425 mm, MO-SCI Corporation) were used as model collectors in transport experiments. Preliminary work showed that consistent and accurate results could only be obtained if the glass beads were properly pretreated. More specifically, good reproducibility required mild sonication in base (0.1 M NaOH), acid (1 M HNO_3), and DI water both upon receipt (prior to drying and storage), and again immediately prior to use. Further details regarding the treatment of the glass beads and the effects of this on reproducibility are provided in SI (see Figure S1, Figure S2, and Table S3 and accompanying discussion). After treatment the beads were kept saturated before and during the column packing process.

Final column packing and preparation was by means of a wet-pack method that was designed to avoid introducing air bubbles into the porous media. Details regarding column preparation and a schematic as well as a photograph are provided in SI (Figure S3). The porosity of the columns was consistently set at 0.38 as calculated from the preset mass and density of the beads and the length and inner diameter of the columns. The pore volume was 9.73 cm^3 for short (5.2 cm) columns and 18.67 cm^3 for long (10.2 cm) columns.

Transport Experiments. A dual-pump system was used for transport experiments (Figure S4). Two feed solutions, one containing DI water ("DI line") and the other containing a sodium chloride or calcium chloride background electrolyte solution ("electrolyte line") were used. For most experiments these solutions were equilibrated with the ambient atmosphere without further pH adjustment (pH = 5.8 ± 0.2), although some solutions were adjusted with the addition of 1.0 M HCl or 1.0 M NaOH to represent acidic (pH = 4.0 ± 0.2) or basic (pH = 10.0 ± 0.2) conditions, respectively. Buffers were avoided to eliminate their possible effects on O-MWCNT attachment efficiency. DI and electrolyte solutions were pumped at constant flow rate (each at 3.5 mL/min) by two peristaltic pumps operating in parallel. Immediately prior to the column inlet, these lines were combined in a custom-built Teflon in-line mixing chamber of <1 mL internal volume that contains a tiny Teflon coated stir bar. Before each experiment, the column was conditioned first with DI water and then with background electrolyte, each for >20 pore volumes. For experiments involving NOM both DI and electrolyte lines included a predetermined concentration of SRNOM.

To introduce O-MWCNTs into the feed solution we used a pulse-input approach. Relative to a step feed, pulse-inputs use a much smaller total mass of O-MWCNT particles so that conditions of clean bed filtration can be more easily maintained. During the pulse-input experiment a 0.6 mL pulse of O-MWCNT dispersion at a concentration of ∼2.0 mg/L was injected into the DI line through an injection loop (Supporting Information, Figure S4). The injection loop approach eliminates unwanted pressure spikes that can sometimes occur with syringe injections. O-MWCNT dispersions at the appropriate pH and NOM concentrations were then added into the DI line (as opposed to the electrolyte line) to minimize any aggregation or deposition prior to entering the column. Mixing of the DI and electrolyte lines occurred immediately prior to solution upflow through the column. For selected columns, separate runs were conducted using pulses of sodium nitrate for an independent measurement of a column's residence time distribution and hydraulic dispersivity. In addition, we employed the step-input method while investigating the spatial distribution profile of 7.1% O-MWCNTs in order to accumulate relatively more O-MWCNTs on the collector surface and to thus achieve more accurate measurement of retained mass. Details regarding the step-input method can be found in the Supporting Information, including Figure S5.

To measure O-MWCNT concentrations in the column effluent, UV absorbance (at λ = 270 nm for O-MWCNTs and 302 nm for $NaNO_3$ tracer) was measured in real time as the effluent passed through a 5-cm path-length flow-through quartz cell (Starna Cells, Inc.) as shown in Supporting Information, Figure S4. The advantage of the long-path-length cuvette (internal volume ≈ 1.2 mL) is that O-MWCNT concentration can be more accurately measured at lower and more environmentally relevant concentrations (<0.25 ppb). For experiments involving SRNOM, effluent concentrations of O-MWCNTs were quantified by measuring absorption at 270 nm with subtraction of the constant background absorbance of NOM at this wavelength. O-MWCNT concentration values in these experiments were also verified using absorbance at 800 nm, where SRNOM does not absorb (Supporting Information, Figure S6). Absorbance at 270 nm was used for the subsequent calculation owing to the higher sensitivity of UV response to concentration changes at this wavelength. The pH of the effluent was also closely monitored (Accumet Engineering Corp.) in all column experiments to ensure that it remained constant.

Prior to each O-MWCNT transport experiment, two preliminary control runs were conducted using the same initial mass of injected O-MWCNTs. The first of these control tests involved a "bypass" run (i.e., at the designated IS but with all flow bypassing the column; Supporting Information, Figures S4 and S5) in order to independently verify the injected mass. The mass estimates from these bypass runs were used to represent injected mass in subsequent data analysis. This mass was also used to calculate the "characteristic" concentration (C_0) for normalization of column effluent concentrations, as shown subsequently in eq 2. The second control test involved the removal of all electrolytes from the feed lines in order to confirm that the measured mass recovered during DI water transport was reproducible and similar to that measured by the accompanying column bypass experiment. Mass recovery relative to the bypass was excellent (100% ± 5%; Supporting Information, Table S4), thus confirming that we could reproducibly measure α = 0 under conditions unfavorable to attachment.

Determination of Spatial Distribution of O-MWCNTs Retained during Transport Experiments. For purposes of qualitatively confirming the presence of first-order deposition, we obtained profiles of the spatial distribution of retained O-MWCNTs for selected experiments, as further described in the Supporting Information. For these experiments, a step-input method was used to increase the recoverable amount of deposited O-MWCNTs. Such profiles were obtained by dissecting the column, separating the porous media into slices of known mass, and determining the mass concentration of O-MWCNTs deposited within each slice. Details regarding the methods used for this spatial analysis can be found in Supporting Information, including Figure S7.

Quantitative Analysis of Column Effluent Data. As confirmed through subsequent experiments conducted using step inputs and evaluation of spatial distributions of O-MWCNTs in our columns, our transport experiments were characterized by good penetration of O-MWCNTs throughout

the column depth. Although detailed numerical evaluation of the spatial concentration data is beyond the scope of the present paper (and the subject of ongoing analysis), our preliminary results are sufficient to show that the majority of CNT removal can be well-characterized by irreversible first-order removal (see Supporting Information for details, and particularly Figure S8).

With the above as justification and also given good fits of model simulations to observed O-MWCNT concentration data (further described subsequently), our quantitative interpretation of transport results was based on an assumption of first-order irreversible deposition, as appropriate for clean-bed filtration in the absence of straining. More specifically, we applied the following one-dimensional advection−dispersion equation [71] toward the estimation of k_d, a first-order coefficient for irreversible loss of O-MWCNTs during transport:

$$\frac{\partial C(x,\,t)}{\partial t} = D\frac{\partial^2 C(x,\,t)}{\partial x^2} - v_p\frac{\partial C(x,\,t)}{\partial x} - k_d C(x,\,t) \quad (1)$$

where C(x, t) [M/L^3] is the aqueous O-MWCNT concentration at position x within the column [L] and time t [T], D is the hydrodynamic dispersion coefficient [L^2/T]; v_p is the pore water velocity in the x direction [L/T], and k_d is the deposition rate coefficient [T^{-1}] for irreversible first-order loss from the pore water. The solution of eq 1 for a column with fixed length is[53]

$$C(t) = C_0\tau\frac{L}{2\sqrt{\pi t^3 D}}\exp(-k_d t)\exp\left[\frac{(L - v_p t)^2}{4Dt}\right] \quad (2)$$

where C_0 is a characteristic concentration defined as M_0/V_{pore}, [M/L^3], M_0 is the mass recovery from the bypass experiment [M], V_{pore} is the aqueous pore volume within the column [L^3], τ is the mean hydraulic retention time ($\tau = V_{pore}/Q$, [T], where Q is the volumetric flow rate of the feed solution [L^3/T]), and L is the column length [L]. For a pulse-input method k_d can be calculated from the fraction of O-MWCNTs that are recovered, as follows:

$$k_d = -\frac{1}{\tau}\ln\left(\frac{Q}{M_0}\int_0^\infty C(t)\,dt\right) \quad (3)$$

The deposition rate coefficient, k_d, reaches a constant maximum value, $k_{d,\,fast}$, at high IS. We estimate this value from experiments conducted at the highest IS. The attachment efficiency α for all other runs can then be calculated using eq 4:

$$\alpha = \frac{k_d}{k_{d,fast}} = \frac{\alpha\eta_0}{\eta_0} \quad (4)$$

Note that the value used for τ does not affect the result so long as it is constant during the experiments where $k_{d,\,fast}$ and k_d are determined.

As an alternate approach, k_d can also be obtained by fitting eq 2 to the effluent concentration data using independent estimates of L, v_p, and D from prior analysis of tracer data. The mass recovery method of eq 3 was used for the subsequently reported results; however, we applied both methods of determining k_d to five columns that represented a wide range of k_d values (Supporting Information, Table S4). In all cases, the fits of the model to the data were generally good (data not shown) and, more importantly, the fitted results were approximately equivalent to those obtained on the basis of mass recovery (Table S4).

A plot of attachment efficiency (α) versus electrolyte concentration on a log−log scale creates an "attachment efficiency curve" and the concentration at which α approaches 1.0 is commonly referred to as the critical deposition concentration (CDC). A quantitative estimate of an approximate CDC can be made by applying the following empirical equation:

$$\alpha = \frac{1}{1 + \left(\frac{CDC}{C_{electrolyte}}\right)^b} \quad (5)$$

where $C_{elctrolyte}$ is the concentration of the background electrolyte (Na^+ or Ca^{2+}) [mg/L] and b is a fitted coefficient equal to the slope of the log−log curve in the reaction limited regime, where $C_{elctrolyte} \ll$ CDC.

RESULTS AND DISCUSSION

Importance of Appropriately Preparing Porous Media. As previously described (and elaborated in Supporting Information), preliminary studies revealed that extensive and standardized methods of glass bead cleaning and packing were required to obtain reproducible column transport data. We hypothesize that this was because the ultrasonic cleaning approach removed small air bubbles and other colloids from the glass bead surfaces, significantly improving the homogeneity of the surface. The presence of colloidal silica in the bead cleaning solution was confirmed using energy dispersive X-ray (EDX) spectroscopy on particle types that were most commonly observed in the wash solution, as determined by visual observation of transmission electron microscopy (TEM) images. See Supporting Information for details, including an example TEM image (Figure S1).

O-MWCNT Transport in the Absence of Deposition. The O-MWCNT transport experiments in DI water exhibited similar shape and average residence time as the $NaNO_3$ tracer (see Figure 1). On the basis of the 100% recovery of O-MWCNTs in DI water and identical values of τ to those determined from tracer studies, we conclude that straining is negligible under the transport conditions tested, that is, at low concentrations of well-dispersed O-MWCNTs and with the relatively uniform glass bead media. Absence of straining has also been observed by others studying CNT transport in well cleaned sands,[56,64,72−74] but other investigators studying some quartz sands and soils have observed CNT retention at zero or low concentrations of background electrolyte and have attributed these observations to straining.[52−55] Clearly, the nature of the media is a critical factor that can control the relative importance of straining toward CNT transport.

Evaluation of O-MWCNT Aggregation during Transport. To evaluate possible in-column aggregation effects, we conducted a series of control experiments with varying masses of injected O-MWCNTs (7.1% O) at two conditions of aquatic chemistry: (a) 5.0 mM NaCl at pH 4.0 and (b) 40 mM NaCl at pH 5.8. The mass range used (1.2 to 12.9 μg O-MWCNTs) was chosen to provide a 10-fold range that included (at the lowest mass) the 1.2 μg mass value used in most experiments. These two aqueous conditions were chosen to obtain attachment efficiencies of about 0.5 to 0.7, where the α value should be most sensitive to any change of the O-MWCNTs condition. Our assumption was that if there was any aggregation and/or straining occurring within the porous media, input concentrations would affect the fractional rate of

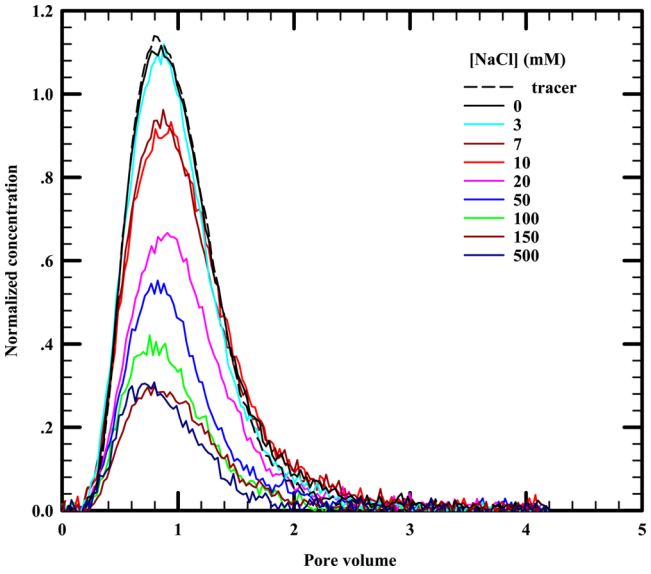

Figure 1. . Illustrative O-MWCNTs transport results for one of the studied materials (7.1% O-MWCNTs) at varying ionic strength. Shown are normalized column effluent concentrations versus number of pore volumes fed for 7.1% O-MWCNTs passing through 5.2 cm long columns at pH 5.8 ± 0.2 under multiple conditions of background NaCl concentration. The normalized concentration is determined as C/C_0, where C_0 is as defined in the text. Fractional mass recoveries for all curves are provided in Table S5 of Supporting Information.

deposition (i.e., k_d) and therefore α. In addition, dynamic light scattering was used to directly measure homo-aggregation rates for 7.1% O-MWCNTs at pH 5.8 ± 0.2 and 4.0 ± 0.2 and for 3.0% O-MWCNTs at pH 5.8 ± 0.2 at multiple ionic strengths—see Figure S10.

Results from evaluation with varying mass (Supporting Information, Figure S9) revealed that, within a 95% confidence interval, the calculated attachment efficiency for 7.1% O-MWCNTs at pH 5.8 and pH 4.0 remained constant even as injected mass increased by over 10-fold. The independently obtained aggregation profiles (Figure S10) show very little aggregation at low IS and offer further insight to these results. At pH 5.8 and IS 40 mM, the particle size of 7.1% O-MWCNTs increased from ~140 nm to ~240 nm during the retention time for a column with a length of 5.2 cm (83.4 s) and increased from ~140 nm to ~300 nm during the retention time for a column with a length of 10.2 cm (163.6 s). The potentially doubled particle size did not have a significant effect on their deposition onto the collectors. Considering the results shown in Supporting Information, both Figures S9 and S10, and although the results are less precise at pH 4.0 than 5.8 (Figure S9), we conclude that the effects of homoaggregation and straining of O-MWCNTs is not substantial under either condition during the full time periods of transport.

Although the mass injection tests at $0.5 < \alpha < 0.7$ do not confirm the complete absence of aggregation (and perhaps straining) where α values are higher, these results provide an important assurance that aggregation and straining are not confounding the results in the column experiments for 7.1% O-MWCNTs at the tested α values and below. This is significant because results under these conditions might be viewed as the principle evidence for subsequent conclusions about the impacts of pH, ionic strength, calcium, and NOM. Moreover, these results, in combination with our independently conducted homoaggregation studies (Supporting Information, Figure S10), also serve as evidence against the significant effect of aggregation and straining for other experiments at similar and lower α-value. This is certainly true for cases with O-MWCTs of higher surface oxygen content, since more highly oxidized O-MWCNTs are more stable against aggregation.

Effect of IS. The effects of IS on O-MWCNT transport are consistent with tenets of the DLVO theory and prior results observed by others.[52,53,64] In particular, the fractional mass recovery of O-MWCNTs in column effluent decreased systematically with increasing NaCl concentration down to a minimum value as the IS approached the CDC (~150 mM NaCl in Figure 1 for example). Fractional removals and computed attachment efficiencies for these and all other reported experiments are provided in Supporting Information, Tables S5–S7. Above the CDC this minimum fractional mass recovery was constant to within experimental error (±5% of C/C_0) as the NaCl concentration continued to increase. This minimum fractional recovery (maximum removal) corresponds to a maximum rate of O-MWCNT deposition in the regime where attachment is favorable (α =1) and fractional rates of deposition are controlled only by physical processes of diffusion and mass transfer. This is more clearly evident when data are interpreted in terms of attachment efficiency as shown in Figure 2 for different O-MWCNTs over a range of different pH values. In this figure, the open triangles in panel b are derived from the transport effluent data shown in Figure 1 (7.1% O-MWCNTs at pH 5.8). Within the unfavorable (below CDC) regime, Figure 2 shows that a 10-fold increase in IS resulted in at least

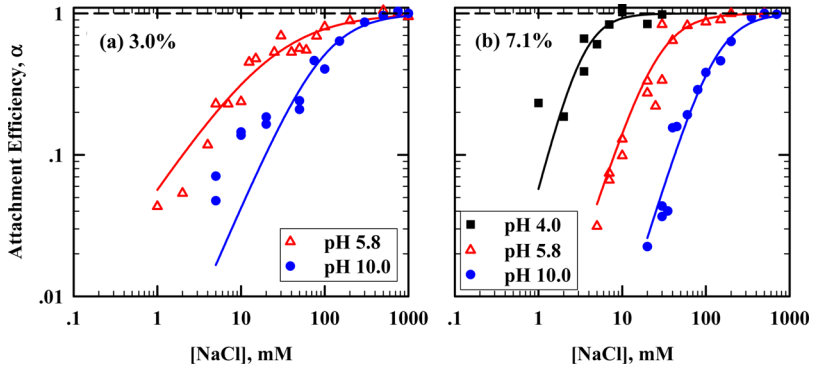

Figure 2. Critical deposition curves for O-MWCNTs with total oxygen concentrations of (a) 3.0% and (b) 7.1%. Results were obtained at pH 10 (filled blue circles), pH 5.8 (open red triangles), and pH 4 (filled black squares).

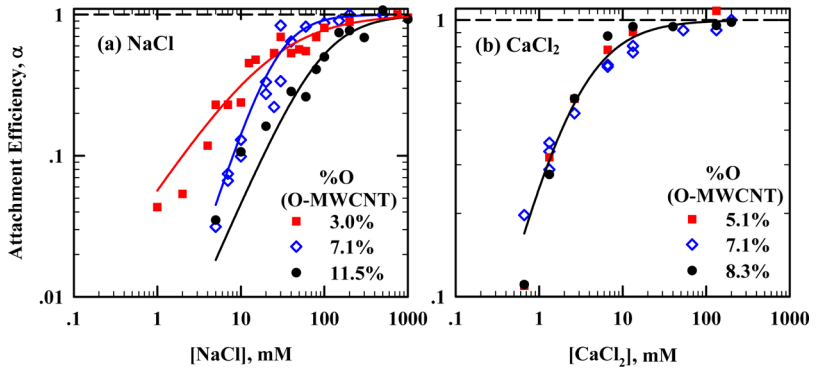

Figure 3. Critical deposition curves of O-MWCNTs with varied surface oxygen concentration at pH 5.8 ± 0.2 in the presence of (a) NaCl and (b) $CaCl_2$ as background electrolytes.

5-fold increases in α for all MWCNTs tested. This observation is different from that of Jasi et al.,[52] who observed that a 10-fold increase in the ionic strength produced only a 2-fold increase in α within the unfavorable deposition regime. We believe that this difference can be ascribed to the presence of straining in the results of Jasi et al. and to the fact that straining should be comparatively insensitive to the effects of ionic strength. We also observed that results for 3.0% O-MWCNTs at lower pH have greater uncertainty than other data in regard to the ionic strength required to obtain a given α (see Figure 2a). The cause of this uncertainty is unknown, but may relate to greater variability among samples at this lower oxidation extent.

Effect of pH. Few researchers have systematically studied the effect of pH on MWCNT deposition.[73] In this paper, the effect of pH on the transport of two different types of O-MWCNTs (3.0% O and 7.1% O) was studied with NaCl as the electrolyte. As shown in Figure 2, the data reveal that CDC values for O-MWCNTs increased systematically with pH between 4.0 and 10.0 for both types of O-MWCNTs. All of the CDC curves could be well fit by eq 4, yielding estimated CDC values for 3.0% O-MWCNTs of 24.4 mM and 96.8 mM at pH 5.8 and 10.0, respectively. CDC values for 7.1% O-MWCNTs were 3.4 mM, 27.3 mM, and 134.4 mM at pH 4.0, 5.8, and 10.0, respectively. As with the previously described IS effects, these results are qualitatively consistent with DLVO theory.[32,33,39] More specifically, reduced barriers to attachment with decreasing pH correspond to the fact that higher proton concentration in solution will lead to a reduced surface charge on both the collectors (glass beads) and particles (O-MWCNTs) due to protonation of negatively charged functional groups, that is, principally carboxyl groups on the O-MWCNTs and silanol groups on the amorphous silica beads. The effect of pH on surface charge for the O-MWCNTs produced in our laboratories is well understood, as previously reported by Smith et al.[21,70] (see Figure 2a in ref 21 and Figure 5 in ref 70). These materials were very similar to those used in our research and were produced by identical methods. Moreover, we also confirmed the presence of a more negative surface charge at higher pH for one of our materials (7.1% O-MWCNTs) by means of zeta potential measurement (see Supporting Information, Figure S11). Unfortunately, however, direct quantitative testing of DLVO theory is not possible for O-MWCNTs owing to the complexities of their shape and size and the unknown aspects of charge distribution on the various interacting surfaces.

Effect of Surface Oxygen on O-MWCNTs. O-MWCNTs with different total surface oxygen concentrations were selected to investigate the effect that surface chemistry has on attachment efficiency during transport. NaCl and $CaCl_2$ were both used separately as background electrolytes in these studies. For the NaCl-based experiments, CDC curves for O-MWCNTs with 3.0% O, 7.1% O, and 11.5% O at pH 5.8 are shown in Figure 3a. Fitting these stability curves to eq 4 yielded CDC values of 24.4, 27.3, and 93.7 mM NaCl, respectively. As previously discussed in the context of Figure 2a, data for 3.0% O-MWCNTs (Figure 3a) show greater uncertainty than do other data, perhaps because of greater variability among samples at this lower oxidation extent. This may also partially explain observed overlap of α-values among O-MWCNTs with 3.0% and 7.1% oxygen at higher NaCl concentrations (Figure 3a), although aggregation and/or straining of either material could also be affecting results in this high α region. In any case, however, the more heavily oxidized O-MWCNTs are clearly more stable toward attachment for conditions at $\alpha < 0.6$ where the possible influence of aggregation and straining can be reliably neglected (see prior discussion of Supporting Information, Figure S9). The data also reveal that CDC is clearly less sensitive to changes in surface oxygen content than to solution pH. This is not surprising in that pH has impacts on surface potential of both the O-MWCNTs and the collectors, whereas changes in surface oxygen only affect the O-MWCNTs.

For experiments conducted with $CaCl_2$ as background electrolyte, CDC curves for three O-MWCNTs are plotted in Figure 3b. In contrast to the obvious effect of surface oxygen concentration on α in NaCl solution, almost no effect was observed in $CaCl_2$ solution. Estimated CDC values for O-MWCNTs at 5.1% O, 7.1% O, and 8.3% O are almost identical at 2.5 mM, 3.0 mM, and 2.4 mM, respectively. As expected, these CDC values are all significantly smaller than those observed in NaCl due to the ability of the divalent calcium ions to more effectively screen the negative surface charges, thereby facilitating attachment. The differences in CDC between Ca^{2+} and Na^{+} based solutions for O-MWCNTs correspond to roughly 9 fold to 39 fold differences, which are substantially less than the 64-fold differences previously observed by Grolimund et al.[71] for spherical carboxylate latex particles and naturally occurring particles during transport through soil. Although the observed difference from Grolimund et al. roughly followed expectations of the empirical Schulze-Hardy rule,[71] we note that the Schulze-Hardy rule was developed from homoaggregation studies and not deposition. Moreover, in light of the relative complexity of O-MWCNT surface charge and morphology we would not necessarily expect these materials

to follow this simple rule. More surprising to us was the lack of CDC dependence on O-MWCNT surface oxygen content when Ca^{2+} was present. Similar effects of the independence of CNT−silica CDC to O-MWCNT surface charge in the presence of Ca^{2+} has also been observed by Yi et al. in their studies of O-MWCNT deposition onto quartz crystal using QCM-D.[43] We follow those authors in suggesting that the existence of multiple Ca^{2+} binding energies with COO^- functional groups on O-MWCNTs (*e.g.*, monodentate or multidentate) could cause a relative insensitivity of CDC to the O-MWCNT surface charge.[43] Note that other authors have also discussed how Ca^{2+} may participate in additional short-range interactions with anionic surfaces such as silica,[75] anionic polymers,[45] and O-MWCNTs.[23,42,76]

Effect of Natural Organic Matter (NOM). The results reported above suggest that O-MWCNTs' attachment efficiencies with amorphous silica can be quite high in clean (organic free) water systems that are mildly brackish (NaCl > 30 mM) or with Ca^{2+} concentrations (>5 mM) commonly found in groundwater environments.[77] Also relevant, however, will be the background dissolved organic matter that is almost ubiquitously present in natural waters. In this regard, it is now widely understood that the presence of NOM can substantially increase particle stabilities and decrease rates of attachment.[42,52,54]

The present investigation builds on the above-noted prior work by providing a more quantitative estimate of fractional deposition rates of O-MWCNTs to amorphous silica under conditions of varying NOM concentration. This was done under carefully controlled conditions of pH and IS using both sodium and calcium chloride as background electrolyte. By determining the deposition rate coefficient, k_d, in the presence of a known concentration of SRNOM and taking the ratio of this value to the previously calculated $k_{d,\,fast}$ (i.e., at the highest Na^+ (500 mM) or Ca^{2+} (132 mM) but in the absence of SRNOM), our work provides a first quantitative metric regarding the effect of SRNOM on α for different types of O-MWCNTs.

As expected, SRNOM was observed to facilitate the transport of O-MWCNTs through glass beads for all three O-MWCNTs studied. Selected (typical) column effluent data for one of the three materials are shown in Figure 4. These results were obtained with 7.1% O-MWCNTs at pH 5.8 and 10 mM $CaCl_2$ over a range of SRNOM concentrations (0−4.1 mg of DOC/L). Also shown for comparison is the O-MWCNT curve obtained at 0.0 IS and a fixed SRNOM concentration of 0.84 mg of DOC/L (dashed line). The 0.0 IS curve is provided for purposes of comparison as a control that has 100% mass recovery (α = 0). The α values obtained through experiments of this type for two O-MWCNTs are plotted as a function of SRNOM concentration (mg DOC/L) in Figure 5 panels a and b, using 5 mM Ca^{2+} and 10 mM Ca^{2+} background electrolyte, respectively. Data for the third less oxidized material (5.1% O-MWCNTs) under these same conditions are provided in Supporting Information, Figure S12. The attachment coefficients under each condition and also under a third electrolyte condition of 100 mM NaCl are detailed in Supporting Information, Table S7.

For all three O-MWCNTs and under all aquatic conditions tested, increasing SRNOM concentration led to decreasing α (i.e., decreasing rates of deposition). With 100 mM NaCl as the background electrolyte, deposition was sensitive to SRNOM as well as O-MWCNT surface oxygen; for example, 0.82 mg of DOC/L of NOM causes a 4-fold decrease in α (from 0.88 to 0.21) for 7.1% O-MWCNTs and a 3-fold decrease (from 0.59 to 0.11) for 8.3% O-MWCNTs (Supporting Information, Table S7).

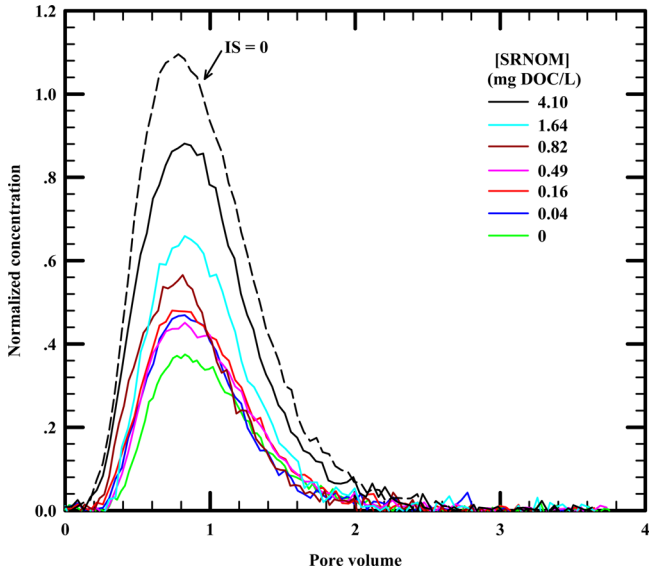

Figure 4. Normalized column effluent concentrations versus number of pore volumes fed for 7.1% O-MWCNTs passing through 5.2 cm long columns at 10 mM $CaCl_2$ and pH 5.8 ± 0.2, under multiple conditions of SRNOM concentration (mg of DOC/L). The dashed line shows a breakthrough curve of O-MWCNTs (SRNOM was present at 0.82 mg of DOC/L for this experiment) in the absence of any added background electrolyte. The normalized concentration is determined as C/C_0, where C_0 is as defined in the text. Fractional mass recoveries for all curves are provided in Table S7 of the Supporting Information.

With $CaCl_2$ as background electrolyte, deposition was sensitive to SRNOM but not to O-MWCNT surface oxygen. For both O-MWCNTs shown in Figure 5 results were almost identical. In the presence of 5 mM Ca^{2+} (Figure 5a), α values for two O-MWCNTs tested decreased sharply for SRNOM concentrations between 0.02 and 0.82 mg of DOC/L; however, the decline of α at higher concentrations of NOM was somewhat more gradual. More specifically, α values dropped from 1.0 to 0.2 with the addition of 0.82 mg of DOC/L, but then gradually decreased thereafter, requiring 4.1 mg of DOC/L for $\alpha \approx 0.1$. For the 10 mM Ca^{2+} scenarios (Figure 5b), the same trend was observed but with α dropping only to 0.6 at very low values of SRNOM and then gradually decreasing only to ~0.2 at 4.1 mg of DOC/L of added SRNOM. Results with the less oxidized 5.1% O-MWCNTs (Supporting Information, Figure S12) show similar trends as discussed above for low DOC values although with much greater variability of results owing to the lower stability of these materials. For these reasons, SRNOM concentrations above 0.82 DOC mg/L were not studied for the 5.1% O-MWCNTs.

We postulate that the rapid drop in α at low NOM concentrations (<0.82 mg of DOC/L) corresponds to monolayer coverage of all available O-MWCNT surfaces. Simple calculations confirm that this is a realistic possibility; with roughly 1.2 μg of O-MWCNTs injected (corresponding to $C_0 = M_0/V_{pore}$ = 0.12 mg/L) and assuming 283.3 m^2 surface area per g MWCNT (based on BET measurement from Cho et al.[23]), we estimate that each milligram of SRNOM DOC would need to occupy only 0.04 m^2. This is much lower than the value

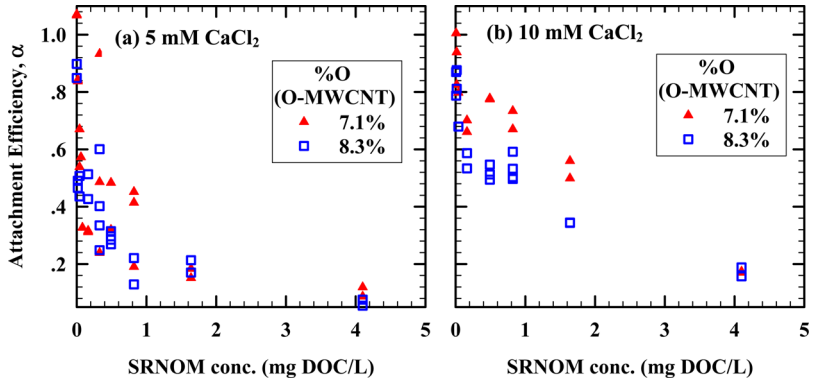

Figure 5. Attachment efficiencies obtained using 7.1% O-MWCNTs (filled red triangles) and 8.3% O-MWCNTs (open blue squares) from transport experiments conducted at pH 5.8 ± 0.2 and in the presence of (a) 5 mM $CaCl_2$ and (b) 10 mM $CaCl_2$ plotted as a function of SRNOM concentration.

of 1 m^2 that has been previously estimated as the amount needed to achieve full monolayer coverage of a mineral surface by moderately sized organic molecules.[78] Thus, our postulation lies well within the realm of possibility. We further postulate that the lower sensitivity of α to DOC at SRNOM concentrations above 0.2 mg of DOC/L reflects a change in dominant mechanism from one of surface charge screening, as the DOC monolayer adsorption blocks the O-MWCNT surfaces to steric interaction as the adsorbed layer of SRNOM thickens.

Considering the effects of surface oxygen on attachment efficiencies in the presence of SRNOM, the results show that such effects were much less substantial in Ca^{2+} based than Na^+ based electrolyte—see Supporting Information, Table S7. These findings are qualitatively similar to those found in the absence of SRNOM (Figure 3b). Moreover, similar effects have been previously reported by Smith et al. who studied homoaggregation in the presence of SRNOM in both simple NaCl solution and in a "synthetic groundwater" containing Ca^{2+}. In that work, as in this, SRNOM dramatically reduced attachment efficiencies in both types of electrolyte, but the impact of surface oxygen was more pronounced in the simple Na^+ solution.[42]

In natural environments where both Ca^{2+} and NOM are present, O-MWCNT transport may be largely independent of O-MWCNT surface oxidation, with attachment efficiencies of dispersed O-MWCNTs being instead controlled primarily by the amount of adsorbed NOM and other aquatic conditions such as pH, ionic strength, and ionic composition. Importantly, the results showed that the presence of even low concentrations of natural organic matter caused low particle attachment efficiencies (α < 0.2) under all conditions tested. Together, these findings suggest that O-MWCNT attachment efficiencies in porous media may be very low in many natural situations where straining is not important, with commensurate implications for deposition. We believe that these findings may be directly relevant for environmental transport under some conditions, such as in subsurface sand and gravel aquifers where grain size and uniformity are sufficient to exclude straining mechanisms.

■ ASSOCIATED CONTENT

Supporting Information

Methodological details for oxidation of MWCTs, characterization of O-MWCNTs, preparation of O-MWCNT dispersions, preparation of glass beads and packed columns, transport experiments using step-input method, determination of spatial distribution of O-MWCNTs retained during transport experiments; O-MWCNTs surface oxygen distribution (Table S1); correlation of UV−vis absorbance and mass concentrations of O-MWCNTs (Table S2); attachment efficiencies of O-MWCNT transport through glass beads treated with different cleaning procedures (Table S3); deposition rate coefficients obtained via two methods (Table S4); fractional mass removal and associated α values obtained under varied experimental conditions (Tables S5−S7); TEM image of supernatant of glass beads after sonication in DI water for one hour (Figure S1); effect of pre-packing treatment for glass beads on the magnitude and precision of attachment efficiency (Figure S2); schematic and picture of packed-bed columns (Figure S3); pulse-input method set-up (Figure S4); step-input method set-up (Figure S5); UV−vis spectra for O-MWCNT dispersion, NOM solution, and a combination of both (Figure S6); UV−vis spectra for O-MWCNT dispersion, Tritan-X 100 solution, and a combination of both (Figure S7); retention profiles of selected column studies (Figure S8); injection mass effect on attachment efficiency (Figure S9); aggregation profile (Figure S10); zeta potential change with pH (Figure S11); Attachment efficiency change of 5.1% O-MWCNTs with varied SRNOM concentrations (Figure S12). This material is available free of charge via the Internet at http://pubs.acs.org.

■ AUTHOR INFORMATION

Corresponding Author

*Phone: (410) 516-5434; e mail: bball@jhu.edu.

Notes

The contents of this work are solely the responsibility of the grantee and do not necessarily represent the official views of the USEPA. Further, USEPA does not endorse the purchase of any commercial products or services mentioned in the publication. The authors declare no competing financial interest.

■ ACKNOWLEDGMENTS

We would like to express our acknowledge to professor Nathalie Tufenkji (Department of Chemical Engineering, McGill University) for her advice and scientific discussion regarding the experimental method of column dissection. We would also like to thank Dr. Kenneth Livi (Department of Earth and Planetary Sciences and Biology, Johns Hopkins University) for his help on TEM analysis. Financial support for

this effort was from the National Science Foundation (Grant No. BES0731147) and the Environmental Protection Agency (Grant No. RD-83385701-1). The contents of this publication are solely the responsibility of the grantee and do not necessarily represent the official views of the USEPA. Further, USEPA does not endorse the purchase of any commercial products or services mentioned in the publication.

REFERENCES

(1) Ebbesen, T. W. Carbon nanotubes. *Annu. Rev. Mater. Sci.* **1994**, *24* (1), 235−264.
(2) Iijima, S. Helical microtubules of graphitic carbon. *Nature* **1991**, *354* (6348), 56−58.
(3) Ebbesen, T. W.; Hiura, H.; Fujita, J.; Ochiai, Y.; Matsui, S.; Tanigaki, K. Patterns in the bulk growth of carbon nanotubes. *Chem. Phys. Lett.* **1993**, *209* (1−2), 83−90.
(4) Dresselhaus, M. S.; Dresselhaus, G.; Eklund, P. C., *Science of Fullerenes and Carbon Nanotubes*; Academic Press: San Diego, CA, 1996; p xviii.
(5) Gallagher, M. J.; Chen, D.; Jacobsen, B. P.; Sarid, D.; Lamb, L. D.; Tinker, F. A.; Jiao, J.; Huffman, D. R.; Seraphin, S.; Zhou, D. Characterization of carbon nanotubes by scanning probe microscopy. *Surf. Sci.* **1993**, *281* (3), L335−L340.
(6) Klaine, S. J.; Alvarez, P. J. J.; Batley, G. E.; Fernandes, T. F.; Handy, R. D.; Lyon, D. Y.; Mahendra, S.; McLaughlin, M. J.; Lead, J. R. Nanomaterials in the environment: Behavior, fate, bioavailability, and effects. *Environ. Toxicol. Chem.* **2008**, *27* (9), 1825−1851.
(7) Parish, A. *Production and Application of Carbon Nanotubes, Carbon Nanofibers, Fullerenes, Graphene and Nanodiamonds: A Global Technology Survey and Market Analysis*; Innovative Research and Products (iRAP), Inc.: Stamford, CT, 2011.
(8) Mueller, N. C.; Nowack, B. Exposure modeling of engineered nanoparticles in the environment. *Environ. Sci. Technol.* **2008**, *42* (12), 4447−4453.
(9) Nowack, B.; Bucheli, T. D. Occurrence, behavior and effects of nanoparticles in the environment. *Environ. Pollut.* **2007**, *150* (1), 5−22.
(10) Petosa, A. R.; Jaisi, D. P.; Quevedo, I. R.; Elimelech, M.; Tufenkji, N. Aggregation and deposition of engineered nanomaterials in aquatic environments: Role of physicochemical interactions. *Environ. Sci. Technol.* **2010**, *44* (17), 6532−6549.
(11) Marrs, B.; Andrews, R.; Pienkowski, D. Multiwall carbon nanotubes enhance the fatigue performance of physiologically maintained methyl methacrylate−styrene copolymer. *Carbon* **2007**, *45* (10), 2098−2104.
(12) Breuer, O.; Sundararaj, U. Big returns from small fibers: A review of polymer/carbon nanotube composites. *Polym. Compos.* **2004**, *25* (6), 630−645.
(13) Vaisman, L.; Marom, G.; Wagner, H. D. Dispersions of surface-modified carbon nanotubes in water-soluble and water-insoluble polymers. *Adv. Funct. Mater.* **2006**, *16* (3), 357−363.
(14) Sluzarenko, N.; Heurtefeu, B.; Maugey, M.; Zakri, C.; Poulin, P.; Lecommandoux, S. Diblock copolymer stabilization of multi-wall carbon nanotubes in organic solvents and their use in composites. *Carbon* **2006**, *44* (15), 3207−3212.
(15) Bourlinos, A. B.; Georgakilas, V.; Zboril, R.; Dallas, P. Preparation of a water-dispersible carbon nanotube-silica hybrid. *Carbon* **2007**, *45* (10), 2136−2139.
(16) Liu, P. Modifications of carbon nanotubes with polymers. *Eur. Polym. J.* **2005**, *41* (11), 2693−2703.
(17) Yusof, A. M.; Buang, N. A.; Yean, L. S.; Ibrahim, M. L.; Rusop, M.; Soga, T. The use of multi-walled carbon nanotubes as possible carrier in drug delivery system for aspirin. *AIP Conf. Proc.* **2009**, *1136*, 390−394.
(18) Li, L.; Xing, Y. Pt−Ru nanoparticles supported on carbon nanotubes as methanol fuel cell catalysts. *J. Phys. Chem. C* **2007**, *111* (6), 2803−2808.
(19) Penza, M.; Cassano, G.; Aversa, P.; Antolini, F.; Cusano, A.; Cutolo, A.; Giordano, M.; Nicolais, L. Alcohol detection using carbon nanotubes acoustic and optical sensors. *Appl. Phys. Lett.* **2004**, *85* (12), 2379−2381.
(20) Savage, T.; Bhattacharya, S.; Sadanadan, B.; Gaillard, J.; Tritt, T. M.; Sun, Y. P.; Wu, Y.; Nayak, S.; Car, R.; Marzari, N.; Ajayan, P. M.; Rao, A. M. Photoinduced oxidation of carbon nanotubes. *J. Phys.: Condens. Matter* **2003**, *15* (35), 5915−5921.
(21) Smith, B.; Wepasnick, K.; Schrote, K. E.; Cho, H. H.; Ball, W. P.; Fairbrother, D. H. Influence of surface oxides on the colloidal stability of multi-walled carbon nanotubes: A structure−property relationship. *Langmuir* **2009**, *25* (17), 9767−9776.
(22) Cho, H. H.; Smith, B. A.; Wnuk, J. D.; Fairbrother, D. H.; Ball, W. P. Influence of surface oxides on the adsorption of naphthalene onto multiwalled carbon nanotubes. *Environ. Sci. Technol.* **2008**, *42* (8), 2899−2905.
(23) Cho, H. H.; Wepasnick, K.; Smith, B. A.; Bangash, F. K.; Fairbrother, D. H.; Ball, W. P. Sorption of aqueous Zn[II] and Cd[II] by multiwall carbon nanotubes: The relative roles of oxygen-containing functional groups and graphenic carbon. *Langmuir* **2010**, *26* (2), 967−981.
(24) Rajagopalan, R.; Tien, C. Trajectory analysis of deep-bed filtration with sphere-in-cell porous-media model. *AIChE J.* **1976**, *22* (3), 523−533.
(25) Yao, K. M.; Habibian, M. M.; Omelia, C. R. Water and waste water filtration—Concepts and applications. *Environ. Sci. Technol.* **1971**, *5* (11), 1105−1112.
(26) McCarthy, J. F.; McKay, L. D. Colloid transport in the subsurface: Past, present, and future challenges. *Vadose Zone J.* **2004**, *3* (2), 326−337.
(27) Tobiason, J. E.; Omelia, C. R. Physicochemical aspects of particle removal in depth filtration. *J. Am. Water Works Assoc.* **1988**, *80* (12), 54−64.
(28) Hahn, M. W.; O'Melia, C. R. Deposition and reentrainment of Brownian particles in porous media under unfavorable chemical conditions: Some concepts and applications. *Environ. Sci. Technol.* **2004**, *38* (1), 210−220.
(29) Elimelech, M.; Omelia, C. R. Effect of particle size on collision efficiency in the deposition of brownian particles with electrostatic energy barriers. *Langmuir* **1990**, *6* (6), 1153−1163.
(30) Veerapaneni, S.; Wiesner, M. R. Role of suspension polydispersivity in granular media filtration. *J. Environ. Eng−ASCE* **1993**, *119* (1), 172−190.
(31) Frimmel, F. H.; von der Kammer, F.; Flemming, H.-C. *Colloidal Transport in Porous Media*; Springer: Berlin, Heidelberg, 2007.
(32) Derjaguin, B. On the repulsive forces between charged colloid particles and on the theory of slow coagulation and stability of lyophobe sols. *Trans. Faraday Soc.* **1940**, *35* (0), 203−215.
(33) Derjaguin, B.; Landau, L. Theory of the stability of strongly charged lyophobic sols and of the adhesion of strongly charged-particles in solutions of electrolytes. *Acta Phys. Chem.* **1941**, *14*, 633.
(34) Elimelech, M.; Omelia, C. R. Kinetics of deposition of colloidal particles in porous-media. *Environ. Sci. Technol.* **1990**, *24* (10), 1528−1536.
(35) Franchi, A.; O'Melia, C. R. Effects of natural organic matter and solution chemistry on the deposition and reentrainment of colloids in porous media. *Environ. Sci. Technol.* **2003**, *37* (6), 1122−1129.
(36) McDowell-Boyer, L. M.; Hunt, J. R.; Sitar, N. Particle transport through porous media. *Water Resour. Res.* **1986**, *22* (13), 1901−1921.
(37) Stumm, W. *Chemistry of the Solid−Water Interface: Processes at the Mineral−Water and Particle−Water Interface in Natural Systems*; Wiley-Interscience: New York, 1992.
(38) Tufenkji, N.; Elimelech, M. Correlation equation for predicting single-collector efficiency in physicochemical filtration in saturated porous media. *Environ. Sci. Technol.* **2004**, *38* (2), 529−536.
(39) Verwey, E. J. W.; Overbeek, J. T. *Theory of the Stability of Lyophobic Colloids*; Elsevier: Amsterdam, The Netherlands, 1948.
(40) Yao, K. M. Influence of suspended particle size on the transport aspect of water filtration. Ph.D. Thesis, University of North Carolina at Chapel Hill, North Carolina, 1968.

(41) Saleh, N. B.; Pfefferle, L. D.; Elimelech, M. Aggregation kinetics of multiwalled carbon nanotubes in aquatic systems: Measurements and environmental implications. *Environ. Sci. Technol.* **2008**, *42* (21), 7963−7969.
(42) Smith, B.; Yang, J.; Bitter, J. L.; Ball, W. P.; Fairbrother, D. H. Influence of surface oxygen on the interactions of carbon nanotubes with natural organic matter. *Environ. Sci. Technol.* **2012**, *46* (23), 12839−12847.
(43) Yi, P.; Chen, K. L. Influence of surface oxidation on the aggregation and deposition kinetics of multiwalled carbon nanotubes in monovalent and divalent electrolytes. *Langmuir* **2011**, *27* (7), 3588−3599.
(44) Qu, X. L.; Hwang, Y. S.; Alvarez, P. J. J.; Bouchard, D.; Li, Q. L. UV Irradiation and humic acid mediate aggregation of aqueous fullerene (nC(60)) nanoparticles. *Environ. Sci. Technol.* **2010**, *44* (20), 7821−7826.
(45) Li, Q. L.; Elimelech, M. Organic fouling and chemical cleaning of nanofiltration membranes: Measurements and mechanisms. *Environ. Sci. Technol.* **2004**, *38* (17), 4683−4693.
(46) Davis, C. J.; Eschenazi, E.; Papadopoulos, K. D. Combined effects of Ca^{2+} and humic acid on colloid transport through porous media. *Colloid Polym. Sci.* **2002**, *280* (1), 52−58.
(47) Chen, K. L.; Elimelech, M. Interaction of fullerene (C-60) nanoparticles with humic acid and alginate coated silica surfaces: measurements, mechanisms, and environmental implications. *Environ. Sci. Technol.* **2008**, *42* (20), 7607−7614.
(48) Chen, K. L.; Mylon, S. E.; Elimelech, M. Enhanced aggregation of alginate-coated iron oxide (hematite) nanoparticles in the presence of calcium, strontium, and barium cations. *Langmuir* **2007**, *23* (11), 5920−5928.
(49) Yoon, S. H.; Lee, C. H.; Kim, K. J.; Fane, A. G. Effect of calcium ion on the fouling of nanofilter by humic acid in drinking water production. *Water Res.* **1998**, *32* (7), 2180−2186.
(50) Iler, R. K. Coagulation of colloidal silica by calcium-ions, mechanism, and effect of particle-size. *J. Colloid Interface Sci.* **1975**, *53* (3), 476−488.
(51) Auset, M.; Keller, A. A. Pore-scale visualization of colloid straining and filtration in saturated porous media using micromodels. *Water Resour. Res.* **2006**, *42*, 12.
(52) Jaisi, D. P.; Saleh, N. B.; Blake, R. E.; Elimelech, M. Transport of single-walled carbon nanotubes in porous media: Filtration mechanisms and reversibility. *Environ. Sci. Technol.* **2008**, *42* (22), 8317−8323.
(53) Jaisi, D. P.; Elimelech, M. Single-walled carbon nanotubes exhibit limited transport in soil columns. *Environ. Sci. Technol.* **2009**, *43* (24), 9161−9166.
(54) Wang, Y. G.; Kim, J. H.; Baek, J. B.; Miller, G. W.; Pennell, K. D. Transport behavior of functionalized multiwall carbon nanotubes in water-saturated quartz sand as a function of tube length. *Water Res.* **2012**, *46* (14), 4521−4531.
(55) O'Carroll, D. M.; Liu, X.; Mattison, N. T.; Petersen, E. J. Impact of diameter on carbon nanotube transport in sand. *J. Colloid Interface Sci.* **2013**, *390*, 96−104.
(56) Liu, X. Y.; O'Carroll, D. M.; Petersen, E. J.; Huang, Q. G.; Anderson, C. L. Mobility of multiwalled carbon nanotubes in porous media. *Environ. Sci. Technol.* **2009**, *43* (21), 8153−8158.
(57) Chen, K. L.; Smith, B. A.; Ball, W. P.; Fairbrother, D. H. Assessing the colloidal properties of engineered nanoparticles in water: Case studies from fullerene C-60 nanoparticles and carbon nanotubes. *Environ. Chem.* **2010**, *7* (1), 10−27.
(58) Hu, H.; Yu, A. P.; Kim, E.; Zhao, B.; Itkis, M. E.; Bekyarova, E.; Haddon, R. C. Influence of the zeta potential on the dispersability and purification of single-walled carbon nanotubes. *J. Phys. Chem. B* **2005**, *109* (23), 11520−11524.
(59) Hyung, H.; Fortner, J. D.; Hughes, J. B.; Kim, J. H. Natural organic matter stabilizes carbon nanotubes in the aqueous phase. *Environ. Sci. Technol.* **2007**, *41* (1), 179−184.
(60) Chen, K. L.; Elimelech, M., ENVR 92-Influence of humic acid on the aggregation kinetics of fullerene nanoparticles in monovalent and divalent electrolyte solutions. *Abstr. Pap. Am. Chem. Soc.* **2007**, *234*.
(61) Chen, K. L.; Elimelech, M. Influence of humic acid on the aggregation kinetics of fullerene (C-60) nanoparticles in monovalent and divalent electrolyte solutions. *J. Colloid Interface Sci.* **2007**, *309* (1), 126−134.
(62) Saleh, N. B.; Pfefferle, L. D.; Elimelech, M. Influence of Biomacromolecules and Humic Acid on the Aggregation Kinetics of Single-Walled Carbon Nanotubes. *Environ. Sci. Technol.* **2010**, *44* (7), 2412−2418.
(63) Hyung, H.; Kim, J. H. Natural organic matter (NOM) adsorption to multi-walled carbon nanotubes: Effect of NOM characteristics and water quality parameters. *Environ. Sci. Technol.* **2008**, *42* (12), 4416−4421.
(64) Wang, P.; Shi, Q.; Liang, H.; Steuerman, D. W.; Stucky, G. D.; Keller, A. A. Enhanced environmental mobility of carbon nanotubes in the presence of humic acid and their removal from aqueous solution. *Small* **2008**, *4* (12), 2166−2170.
(65) Fogden, S.; Verdejo, R.; Cottam, B.; Shaffer, M. Purification of single walled carbon nanotubes: The problem with oxidation debris. *Chem. Phys. Lett.* **2008**, *460* (1−3), 162−167.
(66) Price, B. K.; Lomeda, J. R.; Tour, J. M. Aggressively oxidized ultra-short single-walled carbon nanotubes having oxidized sidewalls. *Chem. Mater.* **2009**, *21* (17), 3917−3923.
(67) Salzmann, C. G.; Llewellyn, S. A.; Tobias, G.; Ward, M. A. H.; Huh, Y.; Green, M. L. H. The role of carboxylated carbonaceous fragments in the functionalization and spectroscopy of a single-walled carbon-nanotube material. *Adv. Mater.* **2007**, *19* (6), 883−887.
(68) Wang, Z. W.; Shirley, M. D.; Meikle, S. T.; Whitby, R. L. D.; Mikhalovsky, S. V. The surface acidity of acid oxidised multi-walled carbon nanotubes and the influence of in-situ generated fulvic acids on their stability in aqueous dispersions. *Carbon* **2009**, *47* (1), 73−79.
(69) Worsley, K. A.; Kalinina, I.; Bekyarova, E.; Haddon, R. C. Functionalization and dissolution of nitric acid treated single-walled carbon nanotubes. *J. Am. Chem. Soc.* **2009**, *131* (50), 18153−18158.
(70) Smith, B.; Wepasnick, K.; Schrote, K. E.; Bertele, A. H.; Ball, W. P.; O'Melia, C.; Fairbrother, D. H. Colloidal properties of aqueous suspensions of acid-treated, multi-walled carbon nanotubes. *Environ. Sci. Technol.* **2009**, *43* (3), 819−825.
(71) Grolimund, D.; Elimelech, M.; Borkovec, M.; Barmettler, K.; Kretzschmar, R.; Sticher, H. Transport of in situ mobilized colloidal particles in packed soil columns. *Environ. Sci. Technol.* **1998**, *32* (22), 3562−3569.
(72) Kasel, D.; Bradford, S. A.; Simunek, J.; Heggen, M.; Vereecken, H.; Klumpp, E. Transport and retention of multi-walled carbon nanotubes in saturated porous media: Effects of input concentration and grain size. *Water Res.* **2013**, *47* (2), 933−944.
(73) Tian, Y.; Gao, B.; Wang, Y.; Morales, V. L.; Carpena, R. M.; Huang, Q. G.; Yang, L. Y. Deposition and transport of functionalized carbon nanotubes in water-saturated sand columns. *J. Hazard Mater.* **2012**, *213*, 265−272.
(74) Mattison, N. T.; O'Carroll, D. M.; Rowe, R. K.; Petersen, E. J. Impact of Porous Media Grain Size on the Transport of Multi-walled Carbon Nanotubes. *Environ. Sci. Technol.* **2011**, *45* (22), 9765−9775.
(75) Sulpizi, M.; Gaigeot, M. P.; Sprik, M. The silica-water interface: How the silanols determine the surface acidity and modulate the water properties. *J. Chem. Theory Comput.* **2012**, *8* (3), 1037−1047.
(76) Chen, C. L.; Wang, X. K. Adsorption of Ni(II) from aqueous solution using oxidized multiwall carbon nanotubes. *Ind. Eng. Chem. Res.* **2006**, *45* (26), 9144−9149.
(77) Briggs, J. C.; Ficke, J. F. *Quality of rivers of the United States, 1975 water year: Based on the National Stream Quality Accounting Network (NASQAN)*; U.S. Geological Survey: Reston, VA, 1977.
(78) Mayer, L. M. Extent of coverage of mineral surfaces by organic matter in marine sediments. *Geochim. Cosmochim. Acta* **1999**, *63* (2), 207−215.